High Field
Terahertz Spectroscopy
of
Optically Excited Gallium Arsenide

James Compeau
Advisor: Dr. Yun-Shik Lee
2015-2016

Abstract:
High field time-domain terahertz spectroscopy (TDS) is used to determine the time dependent transmission and the time-delay and optical-power dependent conductivity of a wafer of gallium arsenide (GaAs). Gallium arsenide is a direct band-gap semiconductor and has potential as a computer processor component. Analysis of the transmission of terahertz (THz) frequencies (10^{12} Hz) through GaAs yields the conductivity of the metal at high strength fields and high frequencies. THz radiation is pulsed into the wafer and is absorbed by free carriers. The transmission of the THz radiation is related to the conductivity of the metal via the thin film Fresnel formula.

It is observed that high power optical excitation lowers transmission of the THz radiation, thus increasing optical power increases the material's conductivity. Positive time delay (optical pulse hitting the wafer after the THz pulse) has shown not to significantly affect the transmission of the THz pulse, or the conductivity of GaAs. A delay of 0.0 ps (optical pulse hitting the wafer at the same time as the THz pulse) slightly increases THz transmission and decreases conductivity from the negative delay. 1.0 ps delay follows the same trend as the 0.0 ps delay. The delay of 3.0 ps slightly decreases transmission of THz radiation from the 2.0 ps delay, and increases conductivity of the wafer.

Table of Contents

Introduction

Semiconductors are widely used in computer components, and with the prevalence and necessity of computers in the modern age, efficiency and speed are becoming even more important. Currently, silicon is the material most widely used as a semiconductor in computer components, but there are some key problems with using silicon as a semiconductor, namely, that silicon is an indirect band gap material [1]. Gallium arsenide, however is a direct band gap material, making it preferable as a semiconductor in high-speed computer components [2]. The high-frequency electron dynamics of gallium arsenide, which is the regime in which high-speed electronics operate, is relatively unexplored, so much testing is needed before it can become a more prominent material in the computer component industry.

This research is designed to study the high frequency, high field electron dynamics in gallium arsenide. The driving electromagnetic wave is a strong terahertz pulse, electromagnetic radiation with a frequency on the order of 10^{12} Hz. The electron dynamics will be studied by controlling the time delay of an optical laser pulse around a terahertz pulse, adjusting the terahertz field strength through the sample, and observing how the time delay and field strength affects transmission. From understanding how different strength optical and terahertz pulses with different time delays affect the transmission of the material, a more in-depth understanding of the material's electron dynamics can be drawn. Specifically, using the Drude model, the transmission of THz radiation is related to the conductivity of the material.

Theory

2.1 The Drude Model
To be able to write the conductivity of gallium arsenide through measuring transmission, a model for the system must be chosen. The model used is the Drude model. The Drude model relies on a statistical look at electrons bouncing off of positively charged "cores", and describes how freely valence electrons can move about the atom [3].

The most fundamental assumptions of the Drude model are that positive charges are attached to much larger particles to compensate for the negative charge of electrons and keep the metal neutral. The model also assumes that, for metals, valence electrons are not bound to atoms, but are free to move about the metal [3]. In Drude's theory, the metallic ions formed by the electrons detaching are the positively charged cores. The charge interaction between the metallic ions and the free electrons are not considered in the Drude model.

With these assumptions, kinetic theory is applied to this "gas" of electrons which moves to a background of immobile metallic ions [3]. Though the charge interactions of the electrons and metallic cores are neglected, the electrons still interact with externally applied electric fields. When an electric field is applied, it causes the electrons to move, inducing a small current. Ohm's law states that the current flowing through a wire is proportional to the potential drop along the wire, and inversely proportional to the resistance of the wire. The resistance of the wire depends on the shape and material of the wire, these characteristics are inherent to the metal and included in the resistivity ρ of the metal. The resistivity is defined as the proportionality constant between **E**, the electric field at a point in the metal, and **j**, the current density that the field induces [3].

$$E = \rho\, j \tag{2.1}$$

In a more kinetic sense, the current density is the total amount of charge moving at a velocity in a particular point on the metal [3]. Thus, where n is the number of electrons moving through the point, $-e$ is the charge of an electron, and v is the average velocity of the electrons,

$$j = -ne\, v \tag{2.2}$$

If there is no electric field applied to the metal, the average velocity of the electrons at any point is zero and so the current density is zero.

If an arbitrary electron has some initial velocity v at time $t = 0$ immediately after a collision with an ion core, it will have an additional velocity $-eEt/m$ from an externally applied electric field. It is assumed that the electron has a random direction after the collision with the core, so v does not contribute to the average velocity of the electron [3]. The average of time t between collisions is defined as τ, the relaxation time. So the average velocity of the electron is

$$v_{avg} = \frac{-e\,E\,\tau}{m} \quad \text{so} \quad j = \left(\frac{ne^2\,\tau}{m}\right)E \tag{2.3}$$

We can now introduce a new property, conductivity, which is simply the inverse of resistivity. If we substitute conductivity into equation (1), and substitute that into equation (3), we get

$$\sigma = \frac{ne^2\,\tau}{m} \tag{2.4}$$

2.2 Thin Film Fresnel Formula
With the Drude model, an optically excited metal can be dealt with via the thin film Fresnel formula for metal films. This formula will supply the relation between the relative transmission of an electromagnetic wave through the optically excited metal and the conductivity of the metal. The formula approximates the optically excited metal as two layers. The first layer is a thin film of metal in which the excited electrons are located. The second layer is a substrate, treated as simply the metal without excited electrons.
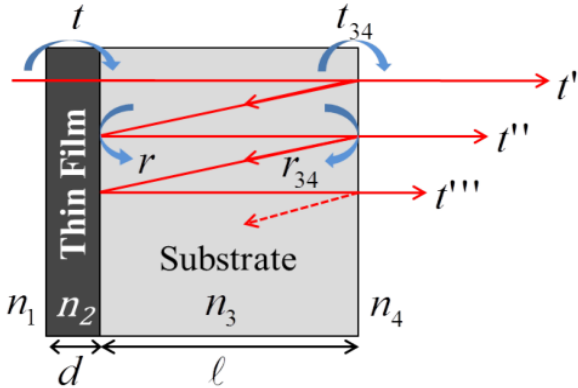

Fig 2.1 Thin Film Approximation [4]
The red lines represent the reflection and
transmission of an incident electromagnetic wave.

Figure 2.1 depicts an incident electromagnetic wave and its propagation through a medium approximated by the thin film Fresnel formula. For the approximation to hold, the thickness of the thin film must be much smaller than the wavelength of light such that the entire transmission through the film can be treated as non-interfering [4]. Conversely, the substrate must be much larger than the wavelength of light such that internal reflections are separated and treated as a "pulse train" and do not interfere [4].

To begin, the normal incidence Fresnel equations model the reflection and transmission through the thin film.

$$r_{ij} = \frac{n_i - n_{i+1}}{n_i + n_{i+1}} \qquad \phi_d = \frac{\omega d\, n_2}{c} = 2\pi \frac{d\, n_2}{\lambda} \tag{2.5}$$

$$t_{ij} = \frac{2 n_i}{n_i + n_{i+1}} \qquad \phi_s = \frac{\omega l\, n_3}{c} = 2\pi \frac{d\, n_3}{\lambda} \tag{2.6}$$

where φ represents the phase change of the wave through the film.
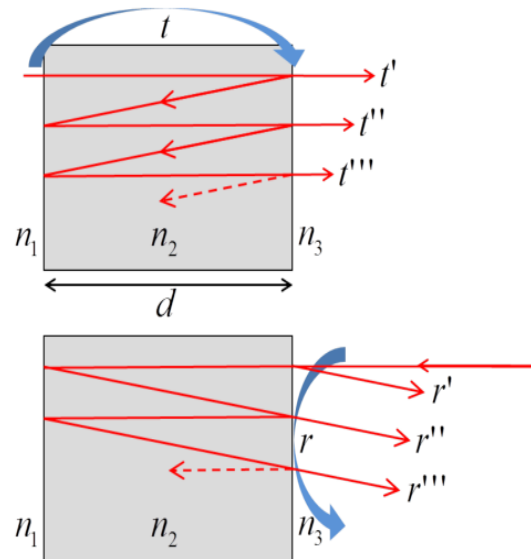

Fig. 2.2 Thin Film Transmission and Reflection Ray Traces [4]
The top image depicts radiation incident on the thin film
and the lower image depicts radiation reflected from the
substrate back into the film

Figure 2.2 represents the terms in equations (5) and (6), with the transmission referring to incident light transmitted by the thin film and reflection referring to light that was reflected by the substrate and then again by the thin film.

A critical feature of thin film reflection and transmission is that each electromagnetic wave passes through the film before they can be considered to interfere ($d << \lambda$) [4]. Usually, thicknesses on the order of $\lambda/10$ is sufficient to ensure that thin film treatment is maintained [4].

Figure 2.2 shows how rays can be summed. A total transmission can be found by adding each transmission component, t^n

$$t = t' + t'' + t''' + \dots \tag{2.7}$$

$$= t_{12} t_{23} e^{i \phi_d} \sum_{n=0}^{\infty} \left(r_{23} r_{21} e^{2i \phi_d} \right)^n \tag{2.8}$$

By applying a geometric series, for $|x| \leq 1$,

$$\sum_{n=0}^{\infty} x^n = \frac{1}{1-x} \tag{2.9}$$

We find

$$t = \frac{t_{12} t_{23} e^{i \phi_d}}{1 + r_{23} r_{12} e^{2i \phi_d}} \tag{2.10}$$

We can now apply the approximations

$$d \ll \lambda \tag{2.11}$$

$$\phi_d \ll 1 \tag{2.12}$$

$$e^{i \phi_d} \approx 1 + i \phi_d \tag{2.13}$$

and for a metal thin-film, we can make the approximations

$$\frac{n_1 n_3}{n_2^2} \ll 1 \tag{2.14}$$

$$n_2 \gg (n_3 - n_1) \gg \frac{n_1 n_3}{n_2} \tag{2.15}$$

Which results in

$$i n_2 \phi_d = 2 \pi i \frac{d}{\lambda} n_2^2 = -Z_0 \sigma d \tag{2.16}$$

Where Z_0 is the impedance of free space. When $\frac{d n_2}{\lambda}$ is small enough that the thin film is a dielectric, the transmission becomes maximum ($t = 1$). For a metal thin film, the metal thin film approximation dominates the transmission coefficient. The small angle approximation holds for thin enough films that the transmission coefficient becomes

$$t = \frac{t_{13} (n_1 + n_3)}{n_1 + n_3 + Z_0 \sigma_s} \tag{2.17}$$

Where σ_s is the conductivity of the metal thin film. Light transmitted through the thin film is then internally reflected by the substrate. The internal reflection is shown by the lower image in Figure 2.2. Treating the reflection similarly to the transmission, we find

$$r=\frac{r_{32}+r_{21}e^{2i\phi_d}}{1+r_{21}r_{32}e^{2i\phi_d}}$$

(2.18)

Applying approximations (2.11-15)

$$r=\frac{n_3-n_1-Z_0\sigma_s}{n_3+n_1+Z_0\sigma_s}$$

(2.19)

To solve the transmission through the substrate, the multiple reflections must be addressed. We will use our assumption that the internally reflected pulses do not interfere. To model relative transmission and intensity, we must find the transmission both with and without the thin film.

$$t_{with}=t\,t_{34}+t\,r_{34}\,r\,t_{34}+t\,r_{34}\,r\,r_{34}\,r\,t_{34}+...$$

(2.20)

$$t_{without}=t_{13}\,t_{34}+t_{13}\,r_{34}\,r_{31}\,t_{34}+t_{13}\,r_{34}\,r_{31}\,r_{34}\,r_{31}\,t_{34}+...$$

(2.21)

Note that t and r are the transmission and reflection from the thin film respectively, and carry all the information from the thin film. To model intensity, we must take the norm-squared of each term.

$$T_{with}=\frac{t^2\,t_{34}^2}{1-r^2\,r_{34}^2}$$

(2.22)

$$T_{without}=\frac{t_{13}^2\,t_{34}^2}{1-r_{31}^2\,r_{34}^2}$$

(2.23)

$$R=\frac{T_{with}}{T_{without}}=\frac{t^2\left(1-r_{31}^2\,r_{34}^2\right)}{t_{34}^2\left(1-r^2\,r_{34}^2\right)}$$

(2.24)

Where R is the relative power transmission. Substituting, we can now rewrite this as conductivity (σ_s) in terms of R

$$\sigma_s=\frac{1}{2\,n_4 Z_0}[\,n_3^2\,2\,n_1\,n_4+n_4^2+\sqrt{\frac{Rn_3^4+2n_3^2\,n_4(2n_1+(2-R)n_4)+n_4^2(4n_1^2+4\,n_1\,n_4+R\,n_4^2)}{R}}\,]$$

(2.25)

Methods

3.1 Terahertz Generation Through Optical Rectification
Non-linear media are capable of changing the frequency of incident radiation. This is known as optical rectification, and is a phenomena that occurs if the electric potential energy of an electron in the medium is asymmetric. This is the phenomena used to generate our THz pulse.

The typical model for an oscillating charge is the harmonic oscillator model. This model represents the charge as a mass on a spring, where the spring's restoring force describes the charge's acceleration and energy. In this case, the restoring force is linear with respect to displacement from equilibrium, and the potential energy is quadratic.

This model assumes that the restoring force of the oscillating electrons can be approximated by a linear force. If the driving EM wave (the wave driving the electron oscillations) is strong enough and the electric potential energy is sufficiently asymmetric, the linear approximation no longer holds [5]. This means that the harmonic oscillator model no longer represents the acceleration.
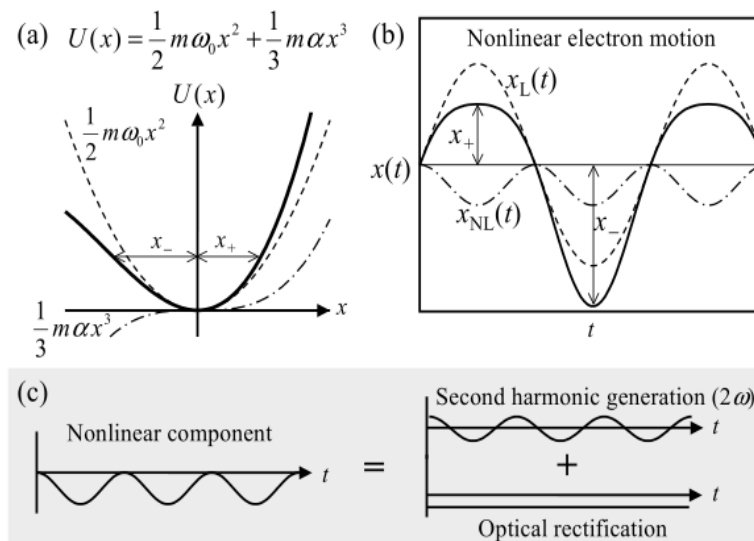

Fig. 3.1 Optical Rectification [5]
(a) shows the potential well of the oscillating charge
(b) shows the oscillation as a function of time
(c) shows the decomposition of the nonlinear portion of the wave form

Under the non-linear regime, approximations of electric potential energy must be made to higher order terms. Fig 1.1(a) shows an example of an electric potential energy that is approximated to the third order. Note that, at small values of x, the second degree approximation (the dashed line) holds well. However, if the displacement is large, the second order approximation no longer holds, and the third order approximation (the dotted and dashed line) must be considered. The sum of the two components of the approximation (the solid line) now appears asymmetric to larger values of displacement. This corresponds to stronger electric fields interacting with this potential in a non-linear fashion.

If driven by a sinusiodal oscillating electric field, the motion of the electron no longer resembles the simple harmonic motion of the original model. Fig 1.1(b) shows the resulting motion of a driven electron in the potential energy shown before. In Fig 1.1(c), the motion is a superposition of a linear component (the frequency component we would expect to see if this were a second order approximation) and a non-linear component. In this case, the non-linear component is itself made of components: a wave that is the second harmonic of the linear motion, and what is essentially a DC electric field signal.

Optical rectification in non-linear media changes the frequency components of the oscillating electron which changes the frequency of the radiation emitted by the accelerating charge. Effectively changing the frequency of of the driving EM wave. It is important to note that the amplitude of the non-linear component is much smaller than the amplitude of the linear component.

Our terahertz radiation is generated via optical rectification through a crystal of lithium niobate (LiNbO$_3$). The nonlinear crystal's properties cause a change in frequency of the incident beam. A small amount of beam intensity becomes THz radiation through each thin layer of the crystal. The optical wave fronts are angled to match the previously generated THz waves, and continuous THz generation resonating with those waves causes an increase in THz power.

The femto-second laser produces a wide-band pulse that hits the lithium niobate crystal. The crystal effects the incident beam non-linearly, and the pulse becomes a superposition of various optical frequencies, and a short THz pulse. At this stage, the THz pulse is not strong enough to elicit a non-linear response from the crystal. Each interaction the optical pulse has with the crystal causes a THz pulse to branch off. This means that, as the optical pulse travels through the crystal, it creates THz waves that interfere with each other. The THz pulse and the optical pulse have different speeds in the material; were the THz pulse and the optical pulse to overlap, there would be a phase difference between the previously and newly generated THz pulses. This phase difference would cause the interference between the two waves to be destructive, and it would destroy the THz pulse.
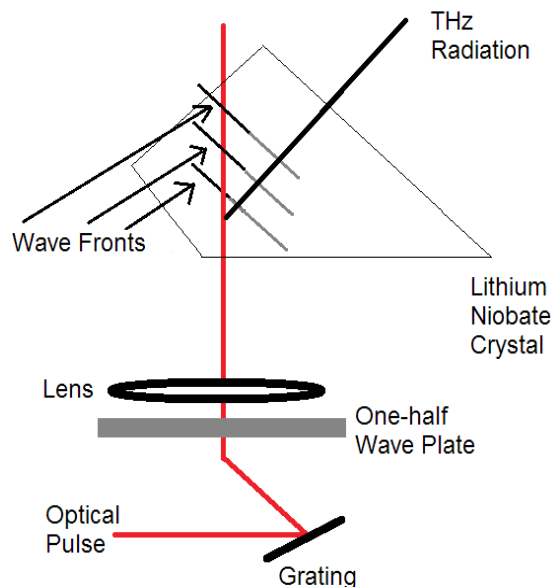

Fig. 3.2 Tilted Femto-second Pulses [5]
Note that angles are not drawn to scale

This is overcome by placing a diffraction grating in the path of the incident optical laser. This diffraction grating will cause a tilt in the optical pulse wave front, and the optical pulse will travel at an angle relative to the THz pulse. This tilt will align the optical and THz wave fronts, and cause the generated THz waves to interfere constructively and increase the power of the THz pulse [5]. This is illustrated in Fig. 3.2 Tilted femto-second Pulse. Note that the wave fronts of the THz and optical pulses align, such that the THz pulse constructively interferes with newly formed THz radiation.

3.2 Terahertz Detection

Terahertz detection is done through a special method of birefringence. Birefringence is a material property in which the polarization and propagation of light through a material changes the index of refraction of the material.

THz pulse   Optical pulse   EO crystal   λ/4 plate   Wollaston prism   Balanced photo-detector

Probe polarization

without THz field

$$I_y = \frac{1}{2} I_0$$

$$I_x = \frac{1}{2} I_0$$

with THz field

$$I_y = \frac{I_0}{2}(1 + \Delta\phi)$$
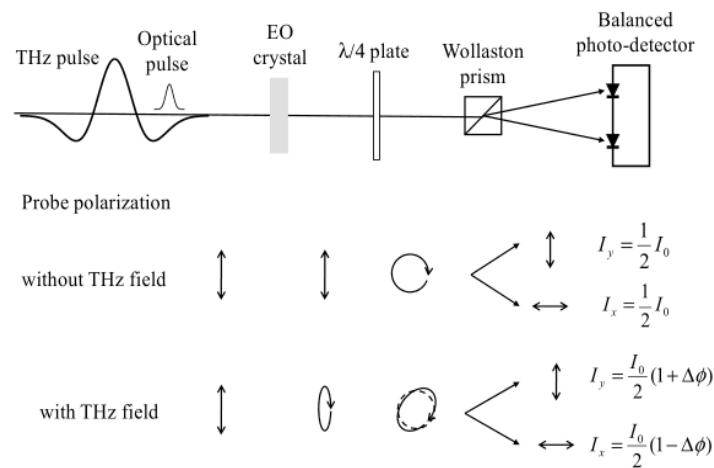
$$I_x = \frac{I_0}{2}(1 - \Delta\phi)$$

Fig. 3.3 THz Detector Setup [5]
Notice that the polarizations
are dependent on the phase of the optical
polarization components

The THz pulse, which is much longer in the position and time domains than the optical pulse, changes the index of refraction of an electro-optic (EO) crystal upon which the optical pulse is incident. With the index of refraction changed, the optical pulse's polarization becomes slightly elliptical. The optical pulse then passes through a quarter wave plate. Normally, the quarter wave plate turns linearly polarized light into circularly polarized light. However, because the optical pulse is already slightly elliptical, the wave plate converts it to an almost circular, but still elliptical polarization. The optical pulse then hits a Wollaston prism, splitting the pulse into orthogonal polarization components and sending it into a balanced photo-detector. Each detector face measures the intensity of the respective polarization, and the relative intensity is based on the strength of the THz field changing the index of refraction of the EO crystal. Figure 2.3 THz Detector Setup [5] shows how the THz field changes the polarization of the optical pulse. Notice that the THz field directly changes the relative phase of the orthogonal components of the optical pulse. This phase difference causes the magnitudes of the components to differ. This difference is directly measured by the balanced photo-detector and then related to the strength of the transmitted THz pulse.

3.3 Terahertz Time Domain Spectroscopy

To measure transmission, an optical breadboard is set up as in Figure 3.4 Optical Table. A laser source beam is initially split and runs down two paths. The beams are designated "THz" and "TDS probe". The TDS probe is guided onto a delay stage. After the beam passes through the stage, it enters a nitrogen purged chamber, then through the sample and into the detector.
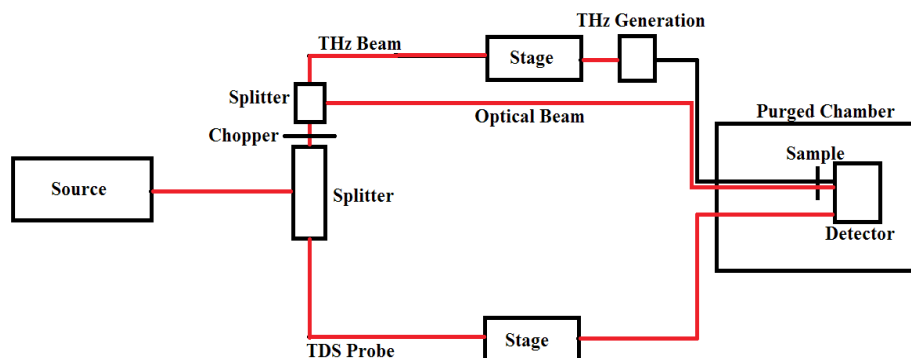

Fig. 3.4 Optical Table
THz generation and THz detection
are explained in detail in sections 3.1 and 3.2

The second beam passes through a spinning chopper wheel that cuts out every other wave pulse, to protect the sensitive detector from overexposure. The beam is split again. The THz beam is guided through another delay stage and then undergoes terahertz generation. Both beams enter a nitrogen purged chamber, and go through the sample into the detector.

THz frequency light is absorbed by water molecules, so the chamber with the sample must be purged with nitrogen and the THz path in air must be short to prevent water molecules from absorbing energy from the terahertz pulse. This purge pushes the air out from the chamber, and prevents the power of the beam from decreasing, providing more stable results. The source beam is generated by a series of four lasers. The resulting beam has a 130 fs pulse. Each pulse is 1 mJ at a repetition rate of 1 kHz and has the output centered at 800 nm, in the infrared band.

The delay stages mentioned are constructed to increase the path length of the beam. Each stage has a pair of mirrors, bending the beam into a "u" shape, with one arm entering the stage, and the other arm exiting in the same direction. With the stages constructed, as above, moving the stage increases the beam length by twice the displacement of the stage. The two stages are controlled by the computer to alter the path length of their respective beams. Using the stages, the terahertz and optical pulses can be centered in time such that $t = 0$ is defined as the time at which the peak of the terahertz pulse hits the detector. The stage along the TDS probe path is responsible for detecting the THz pulse as explained in section 3.2 Terahertz Detection

Before continuing, each path is aligned. Each mirror passes the beam through an iris that is used for alignment. The mirrors are adjusted such that the laser passes through the small, partially closed apertures of the irises. There are many pairs of mirrors and irises, so they are not shown.

There are also translational stages that control the position of the sample in three dimensions. Once the terahertz pulse is centered in time, a small blade is put in place of the sample. The transmission of the terahertz pulse is scanned over the position of the blade in order to find and record the minimum beam waist. With the position of the stage now fixed, the blade is removed and the terahertz pulse and TDS probe are applied. To map the entire THz pulse, the path length of the TDS probe is adjusted by the program so the transmission is measured over points before and after $t = 0$. This is done by scanning the TDS probe over the THz pulse.

Once the test pulse is successfully mapped, the sample is placed in the stage. The program then applies the terahertz pulse, optical beam and TDS probe. The transmission of the terahertz pulse is measured, by scanning the TDS probe over the entire terahertz pulse. The optical beam is is fixed relative to the terahertz pulse, such that the time delay of the optical pulse hitting the sample relative to the terahertz pulse is preserved throughout the scan. Once the scan is finished, the time delay of the optical pulse is changed and the terahertz transmission is scanned again. After several delays are measured, the optical power is changed, and the terahertz transmission is scanned again over the same delays. This will result in a terahertz transmission that illustrates time dependence, and can be compared against different optical powers.

Results & Discussion
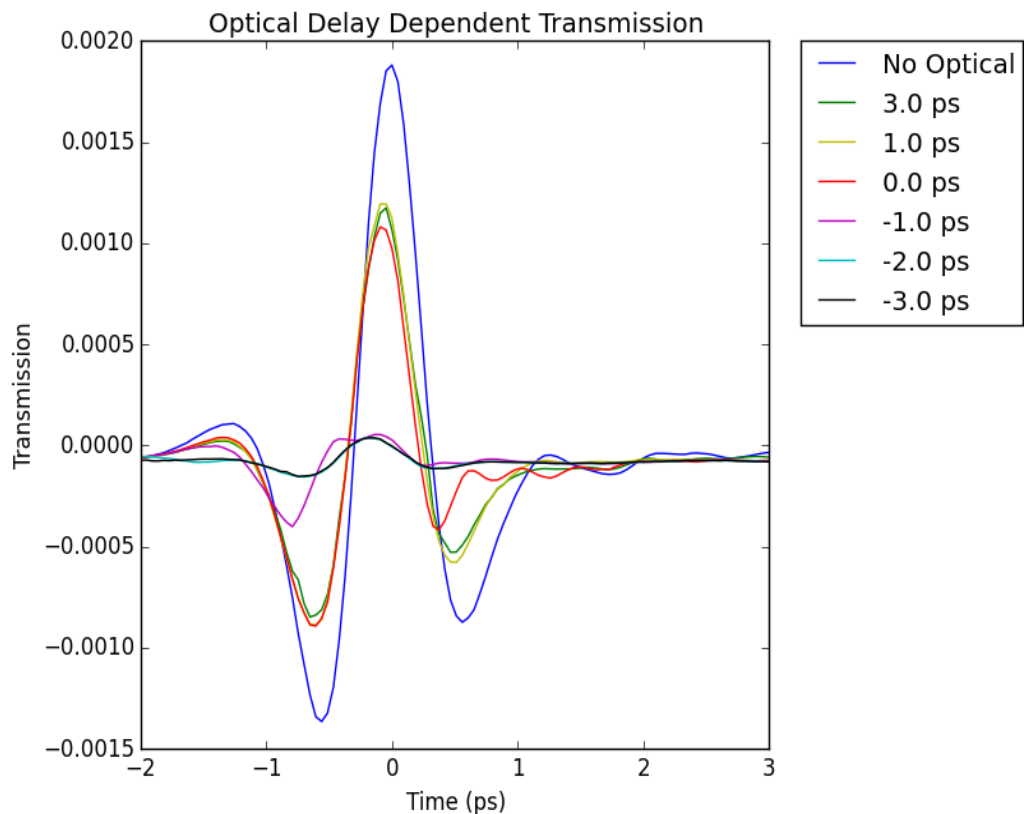
4.1 Transmitted Wave Forms

Figure 4.1 Optical Delay Dependent
Transmission
This plot shows the delay dependent
transmission
of a THz pulse through the GaAs wafer
at an optical power of 2.41 µJ

As expected, the THz pulse on the sample that is not optically excited has much higher transmission than those incident on an optically excited sample. Interestingly, at the peak at 0.0 ps, the THz pulse incident on the sample optically excited at a 1.0 ps delay has a higher transmission than the pulse on the sample with a 3.0 ps delay. I would expect that a longer delay (that is, a larger, positive delay where the optical pulse hits the sample after the THz pulse) would have larger transmission. However, the difference in transmission is marginal and may be due to experimental error. We also see very little transmission from the THz pulses with the -1.0, -2.0, and -3.0 ps delayed optical pulses. The -2.0 ps delay is very nearly on top of the -3.0 ps delay line, and the two are indistinguishable in Figure 4.3.
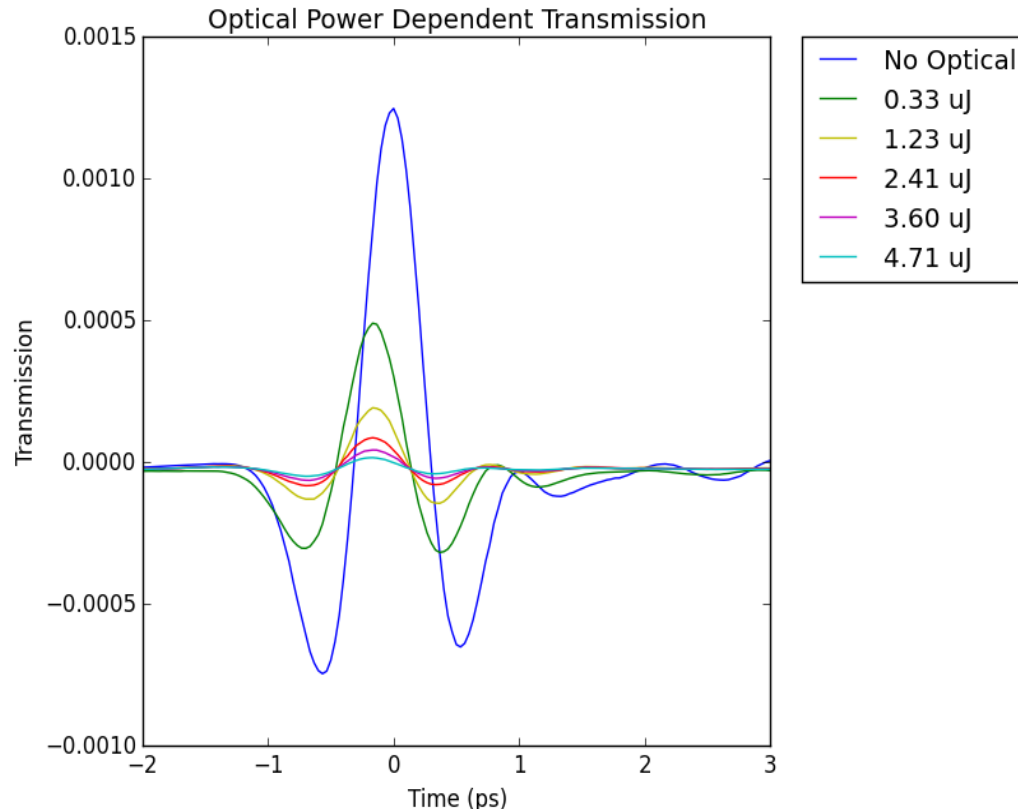

Fig. 4.2 Optical Power Dependent Transmission
This graph represents the relative transmission of the THz pulse at a
particular optical time delay.

Figure 4.2 depicts the relative transmission of the THz pulse at a particular THz power and delay. Similarly to the graphs depicted in figure 3.1, the relative transmission decreases if the optical power increases. Though we do not see the grouping that was shown in figure 4.1, there is still a large difference in transmission between the THz waves with 0.33 μJ and the 1.23 μJ optical pulses, while the difference in transmission between THz waves with 1.23 μJ and 2.41 μJ pulses is much less dramatic.

4.2 Analysis

Ultimately, the goal is to find the conductivity of GaAs as a function of optical pulse delay with a fixed optical power, and to find the conductivity as a function of the optical power at a fixed optical pulse delay. In order to do this, a Fourier transform is applies to the data in figures 4.1, 4.2, and 4.3. Taking the Fourier transform will provide the transmission spectrum of the THz pulse. To find the power spectrum, the transmission spectrum is squared. To normalize the power spectra, the power spectrum of the THz pulse without the optical pulse is integrated. The power spectra are then divided by the spectrum of the THz pulse without the optical pulse.

$$E(x) \rightarrow E(v) \tag{32}$$

$$I = |E(v)|^2 \tag{33}$$

$$I_0 = |E_0(v)|^2 \tag{34}$$

$$I'_0 = \int_{-\infty}^{\infty} |E_0(v)|^2 \, dv \tag{35}$$

$$I' = \int_{-\infty}^{\infty} |E(v)|^2 \, dv \tag{36}$$

$$T = \frac{I}{I_0} \tag{37}$$

$$T(v) = \frac{I'}{I'_0} \tag{38}$$

Where E is the transmission spectrum of the THz pulse undergoing analysis, I is that pulse's power spectrum, I' is that pulse's total power, v is the frequency, and $T(v)$ is the normalized power transmission of the pulse, T is the relative transmission spectrum of the THz pulse through the wafer, E_0 is the transmission spectrum of the THz pulse through the wafer without optical excitation (the baseline measurement), I_0 is the power spectrum of the air reference, and I'_0 is the total power of that pulse.
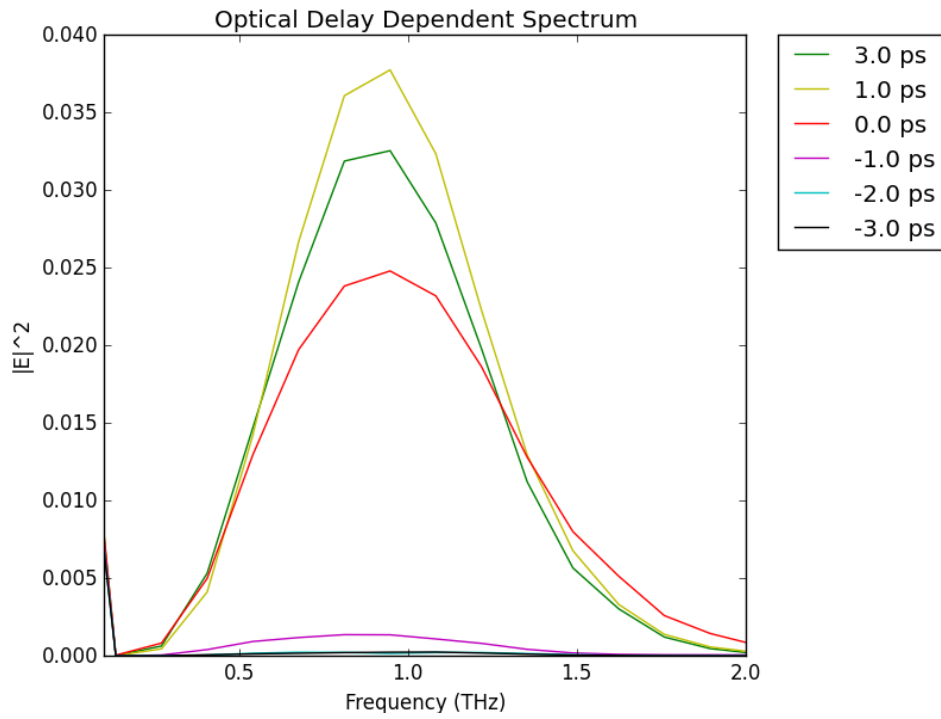
Fig. 4.3 Optical Delay Dependent Spectrum
The spectrum for a THz pulse incident on
a wafer of GaAs that has been excited
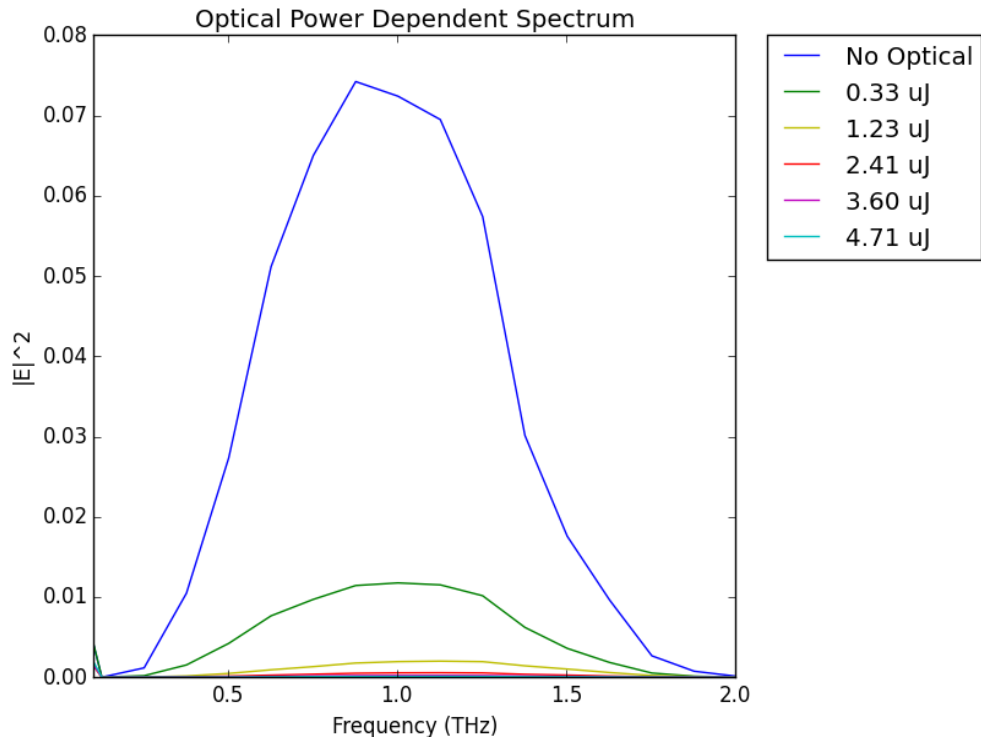by optical pulses of varying
time delays.

Fig 4.4 Optical Power Dependent Spectrum
The power spectrum of the THz wave incident
on
the GaAs wafer with varying optical excitation
powers.

Figures 4.4 and 4.5 show the squared, normalized Fourier transform of the data presented in figures 4.2 and 4.3. The Optical Power Dependent and optical time delay dependent Spectra show several smooth bands that all peak around 1.0 THz.
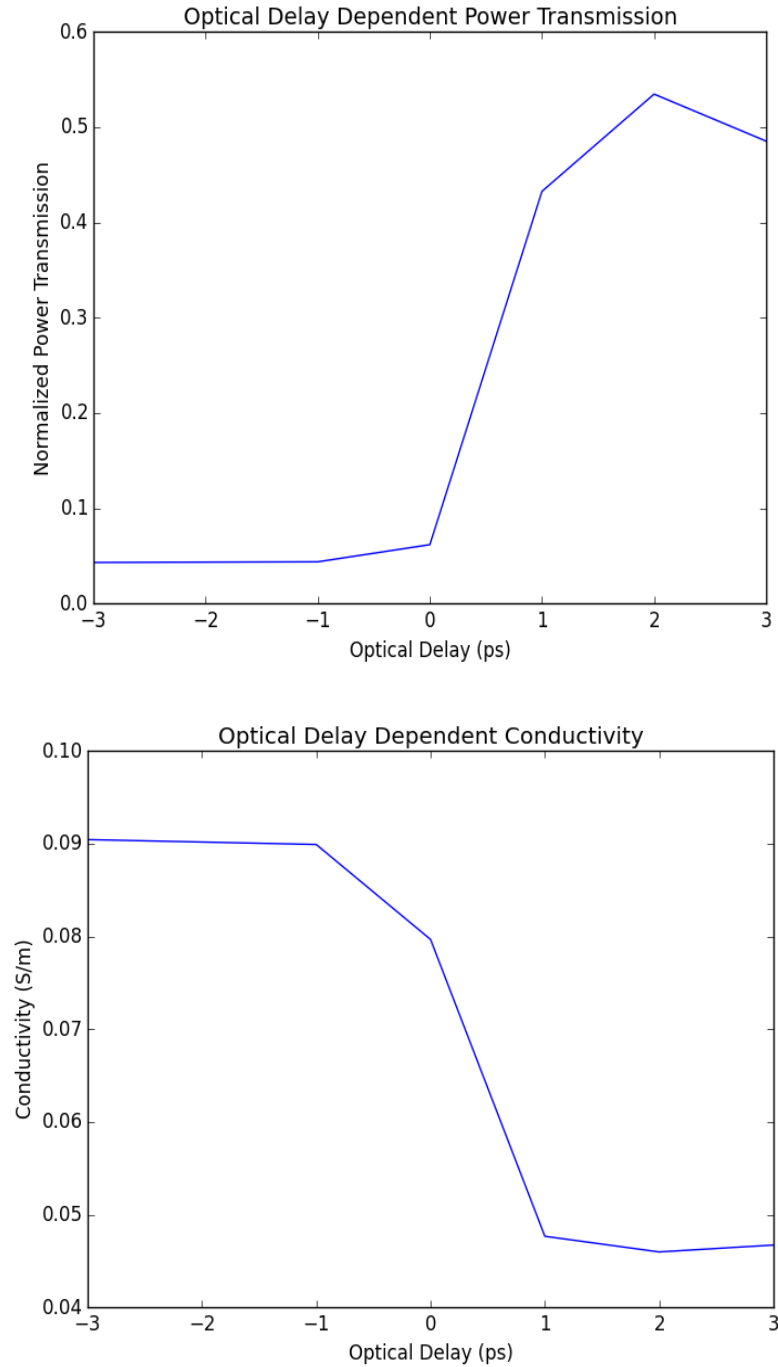

Fig. 4.5 Delay Dependent Transmission
and Conductivity
Transmission and conductivity share a
distinct inverse relation.
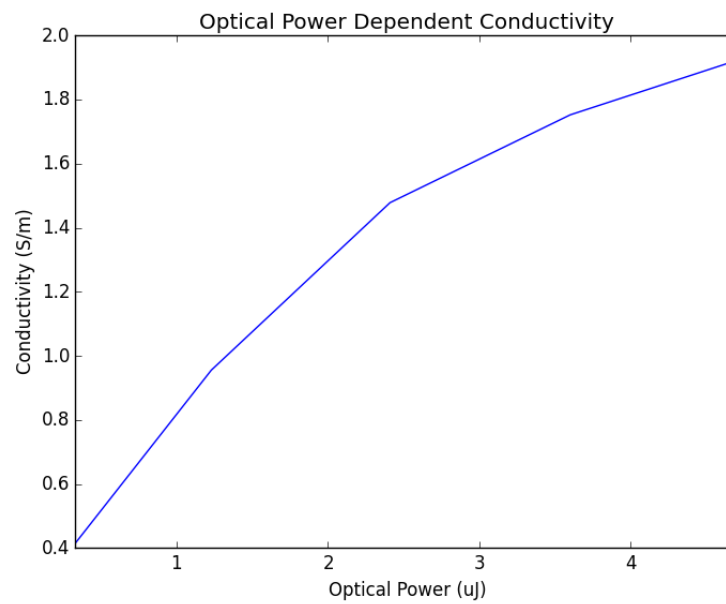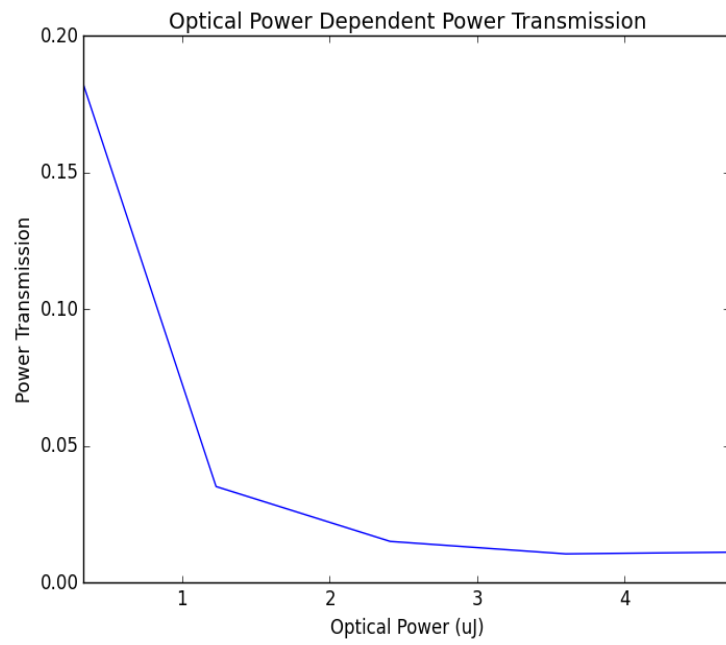Low transmission means high conductivity
and vice versa.

Fig 4.6 Optical Power Dependent
Transmission Conductivity
The inverse relation apparent in figure 4.6
is also apparent here.

The figure 4.6 shows that, in the negative delay regime, transmission is very low. The negative delay means that the optical pulse hits the wafer before the THz, so the optical pulse excites electrons which then absorb energy from the THz pulse. At 0.0 ps delay, the transmission is slightly higher than the transmission in the negative regime, this is because the peak of the optical pulse is centered on the peak of the THz pulse. The optical pulse is much shorter in the time domain than the THz pulse, so the optical pulse is exciting the material after a small amount of the THz pulse has already passed.

The optical delay dependent conductivity in figure 4.6 shows that conductivity in the wafer is much higher the more negative the delay is, dropping off at 0.0 ps delay, and remaining steady at long, positive delays. As above, the negative delay means the optical pulse is hitting the wafer before the THz pulse. The optical pulse will excite the electrons into a conductive state, which is the effect being measured by the THz pulse. At positive delays, the data shows a much lower conductivity, which holds with transmission being lower. If transmission is low, THz power is not being appreciably absorbed, so there are fewer free carriers, hence the low conductivity.

Optical power dependent power transmission, as shown in figure 4.7, displays what appears to be an exponential decay in transmission as optical power increases. It is expected that increased optical power would cause a decrease in transmission; as optical power increases, more electrons are excited into the conductive state. More THz power would be absorbed by the free electrons, causing a decrease in THz transmission. An exponential decay would likely cause an asymptote at zero transmission, as it would make no physical sense for transmission to become negative.

The conductivity of the wafer behaves as the transmission would imply, conductivity increasing as optical power increases. Similarly to the transmission, the conductivity begins to increase more slowly as optical power increases. This is probably a result of the asymptotic behavior of the transmission. If higher optical power could be achieved, and this behavior is due to the nature of the transmission, then there would be a limit to the conductivity of GaAs.

4.3 Conclusion
The conductivity matches predictions from transmission data. Conductivity decreases to near zero with increasing delay, where negative delay is the optical pulse hitting the wafer before the THz pulse. This means the optical pulse hitting the wafer excited carriers that interact with the THz wave. If the delay is higher and positive, the carriers that are excited do not interact with the THz pulse. If more data were taken at negative delays, relaxation time could be determined by looking at how early the excitation pulse must hit the wafer to reduce conductivity to near zero.

Conductivity as a function of optical power increases and seems to increase more slowly with very high optical power. This almost certainly arises from the asymptotic behavior of the transmission. A higher power optical pulse excites more carriers. However, increasing optical power will become less efficient at exciting carriers.

[1] Kane, E. O. "Band Structure of Silicon from an Adjusted Heine-Abarenkov Calculation."*Physical Review* 146.2 (1966): 558–567. Web. 20 Oct. 2015.

[2] Blakemore, J. S. "Semiconducting and Other Major Properties of Gallium Arsenide."*Journal of Applied Physics*53.10 (1982): R123–R181. Web. 20 Oct. 2015.

[3] Ashcroft, Neil W., and N. David. Mermin. *Solid State Physics*. New York: Holt, Rinehart and Winston, 1976. Print.

[4] Paul, Michael Jason. *Nonlinear Terahertz Spectroscopy of Carbon Nanomaterials and Semiconductor Nanostructures*. PhD diss., 2014.

[5] Lee, Yun-Shik. *Principles of Terahertz Science and Technology*. Springer, 2009. Print.